

PHASE-ONLY POSITIONING IN DISTRIBUTED MIMO UNDER PHASE IMPAIRMENTS: AP SELECTION USING DEEP LEARNING

Fatih Ayten¹, Musa Furkan Keskin², Akshay Jain³, Mehmet C. Ilter¹, Ossi Kaltiokallio¹,
Jukka Talvitie¹, Elena Simona Lohan¹, Mikko Valkama¹

¹Department of Electrical Engineering, Tampere Wireless Research Center,
Tampere University, Finland

²Department of Electrical Engineering, Chalmers University of Technology, Sweden

³Radio Systems Research, Nokia Bell Labs, Espoo, Finland

ABSTRACT

Carrier phase positioning (CPP) can enable cm-level accuracy in next-generation wireless systems, while the recent literature shows that accuracy remains high using *phase-only measurements* in the emerging distributed multiple-input multiple-output (D-MIMO) networks. However, the impact of phase synchronization errors on such systems remains insufficiently explored. To address this gap, we first show that the proposed hyperbola intersection method achieves highly accurate positioning even in the presence of phase synchronization errors when trained on appropriate data reflecting such impairments. We then introduce a deep learning (DL)-based D-MIMO antenna point (AP) selection framework that ensures high-precision localization under phase synchronization errors. Simulation results show that the proposed framework improves positioning accuracy compared to prior art methods, while reducing inference complexity by approximately 19.7%.

Index Terms— Carrier phase positioning, distributed MIMO, deep learning, AP selection, phase synchronization errors.

1. INTRODUCTION

Carrier phase-only positioning represents a distinct approach where localization is performed exclusively using carrier phase observations, without relying on complementary measurements such as time-of-arrival (ToA) or time-difference-of-arrival (TDoA). Unlike conventional hybrid schemes that treat carrier phase as an auxiliary source of information, this paradigm leverages the fine-grained phase data as the sole input for estimating the user equipment (UE) position [1, 2, 3]. Such a setting introduces both opportunities for achieving sub-centimeter accuracy and challenges due to the inherent integer ambiguity problem [4, 5] and sensitivity to hardware impairments [6]. Recent studies in distributed and phase-coherent multiple-input multiple-output (MIMO) systems have begun exploring this concept, highlighting its potential for next-generation cellular positioning [4, 7].

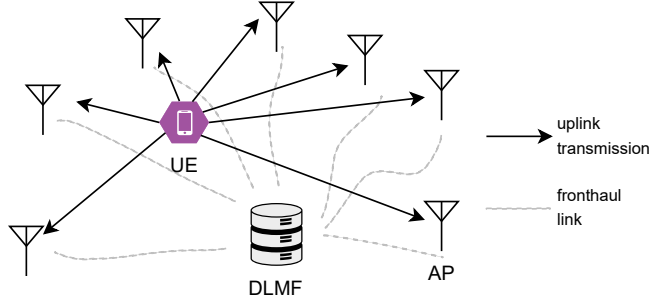


Fig. 1: Uplink UE positioning in a distributed AP deployment, where only carrier phase measurements are taken into account for positioning.

However, practical distributed multiple-input multiple-output (D-MIMO) deployments are inherently affected by phase synchronization errors across distributed antenna points (APs), which significantly degrade performance [8]. In addition, a wide range of applications in next-generation wireless networks must satisfy strict latency requirements [9], which can be alleviated by reducing model complexity.

Motivated by the aforementioned challenges, in this paper, we propose a learning-based location management function (LMF) that leverages deep neural networks (DNNs) to maintain robustness against such impairments. Furthermore, our framework incorporates adaptive AP selection strategies, leveraging received signals and deployment geometry. Extensive numerical evaluations confirm that the proposed deep learning (DL)-based distributed location management function (DLMF) achieves high-precision localization in realistic 6G deployment scenarios, even under challenging phase synchronization errors, with reduced complexity.

2. SYSTEM ARCHITECTURE

The LMF is the key enabler for positioning purposes in 5G New Radio (5G NR), and it can be used to determine the position of a UE utilizing measurements [10]. The DLMF extends the traditional LMF by moving certain positioning

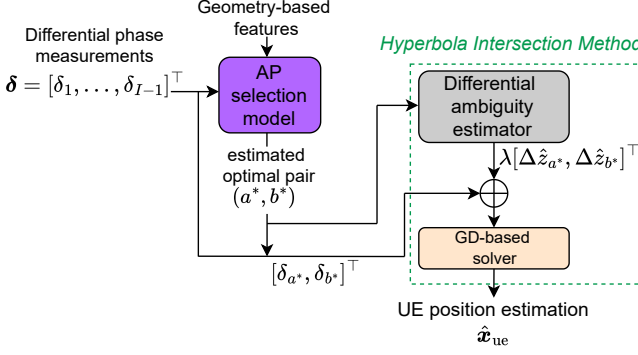


Fig. 2: Block diagram of the proposed phase-only positioning approach.

tasks closer to the UE, reducing latency and improving accuracy [11]. While a central LMF may still coordinate overall operations, the DLMF boosts performance through localized processing. In this work, we assume a D-MIMO system for UE positioning, coordinated by a DLMF unit, as shown conceptually with seven APs in Fig. 1.

Similar to [12, 13, 14], we study an uplink configuration involving I spatially distributed APs. The UE is located at an unknown position $\mathbf{x}_{\text{ue}} \in \mathbb{R}^2$, while the positions of the APs are known and denoted as $\mathbf{x}_{\text{ap},i} \in \mathbb{R}^2$ for $i \in \{0, \dots, I-1\}$. Our analysis focuses on line-of-sight (LoS) propagation. Extensions to multipath environments and three-dimensional positioning remain important directions for future work.

The UE transmits a narrowband pilot signal. The phase of the received signal at the i -th AP is modeled as $\theta_i = -\frac{2\pi}{\lambda}d_i + \gamma_i + \phi_{\text{ue}} + 2\pi z_i + n_i$, where λ is the wavelength, $d_i = \|\mathbf{x}_{\text{ue}} - \mathbf{x}_{\text{ap},i}\|$ is the Euclidean distance, $\gamma_i \sim \mathcal{N}(0, \sigma^2)$ represents the phase perturbation between the DLMF and the i -th AP, ϕ_{ue} is the phase offset between the UE and the DLMF, $z_i \in \mathbb{Z}$ is the integer ambiguity, and $n_i \sim \mathcal{N}(0, \nu_i^2)$ models the phase measurement noise. We assume γ_i and n_i are independent.

One AP (e.g., $i = 0$) is designated as the reference by the network. The corresponding differential measurements for $m \in \{1, \dots, I-1\}$ are then defined as

$$\delta_m = -\frac{\lambda}{2\pi}(\theta_m - \theta_0) = \Delta d_m + \Delta \gamma_m - \lambda \Delta z_m + \Delta n_m \quad (1)$$

where $\Delta d_m = d_m - d_0$, $\Delta \gamma_m = (\lambda/2\pi)(\gamma_0 - \gamma_m)$, $\Delta z_m = z_m - z_0$, and $\Delta n_m = (\lambda/2\pi)(n_0 - n_m)$. Stacking the differential measurements in (1) yields $\delta = [\delta_1, \dots, \delta_{I-1}]^T$.

Each δ_m geometrically corresponds to a set of hyperbolas parameterized by Δz_m , with foci located at $\mathbf{x}_{\text{ap},m}$ and $\mathbf{x}_{\text{ap},0}$.

3. PHASE-ONLY POSITIONING

In this section, we introduce phase-only positioning with AP selection, which integrates DL and gradient descent (GD) techniques to perform positioning. The overall framework is illustrated in Fig. 2. The hyperbola intersection method, originally introduced in [13], is adopted as the underlying localization

model. The proposed DL-based AP selection approach identifies the optimal pair of ambiguities that minimizes the UE positioning error.

3.1. Hyperbola Intersection Method

This method comprises two primary components: (1) a *differential ambiguity estimator* implemented using a multi-layer perceptron (MLP), and (2) a *GD-based solver*. Due to space limitations, a detailed description of the method is omitted; readers are referred to Sec. III of [13] for a similar underlying approach.

The *differential ambiguity estimator* produces the vector of estimates $\Delta \hat{z} = [\Delta \hat{z}_{j_1}, \dots, \Delta \hat{z}_{j_{|\mathcal{J}|}}]^T$ from the differential measurements δ , where $\mathcal{J} = \{j_k\}_{k=1}^{|\mathcal{J}|} \subseteq \{1, 2, \dots, I-1\}$ denotes the set of AP indices for which differential ambiguities are estimated, and $|\cdot|$ is the cardinality. Here, $\Delta \hat{z}_{j_k}$ represents the estimate of Δz_{j_k} . The total number of possible labels across all differential ambiguities is expressed as Q , which depends on the AP positions. The estimated ambiguities $\Delta \hat{z}$, scaled by λ , are added to the differential phase measurements δ to obtain the differential distance estimates $\Delta \hat{d}$.

The *GD-based solver* iteratively refines the UE position estimate using differential distance estimates $\Delta \hat{d}$. At each step, differential distances at the current estimate are computed. A quadratic cost function is then evaluated, and the position is updated with a learning rate of α . After T iterations, the final position estimate \hat{x}_{ue} is obtained.

3.2. Proposed AP Selection Method

For any unordered pair of differential ambiguities $(\Delta z_a, \Delta z_b)$ with $a, b \in \{1, \dots, I-1\}$ and $a \neq b$, the intersection of the corresponding hyperbolas yields a unique UE position estimate. As shown in [13], the computational complexity of the hyperbola intersection method grows with the number of estimated ambiguities, making two-ambiguity localization, i.e., $|\mathcal{J}| = 2$, computationally more efficient. The operation of estimating only two of all possible ambiguities is performed as follows: the shared layers of the ambiguity estimator model in [13] remain active, and only the parallel branches corresponding to those ambiguities are activated, since each branch of the model produces an ambiguity estimate. However, the optimal pair $(\Delta z_a, \Delta z_b)$ may depend on factors such as received signal-to-noise ratio (SNR) and AP geometry. To address this, we propose a neural network (NN)-based approach to identify the pair that maximizes positioning accuracy.

We consider two classes of features: measurement-based and geometry-based. *Measurement-based features* include (1) the differential phase measurements δ and (2) the SNR values (in dB) at each AP. Here, SNR quantifies only measurement noise and excludes phase perturbation variance. To ensure consistent feature dimensionality, an additional zero-valued element is appended to δ for the reference AP, since δ is defined only for $m \in \{1, \dots, I-1\}$. *Geometry-based features*, in turn, capture deployment-specific characteristics of the AP configuration. For each AP in the system, we extract the

following geometric relationships: (1) distance to the reference AP, (2) the angle between the current AP and the reference AP, (3) index of the closest neighbor AP, (4) the angle between the current AP and its closest neighbor AP, (5) index of the farthest AP, and (6) the angle between the current AP and the farthest AP. For each AP, the measurement-based and geometry-based features are concatenated into a vector of dimension 8. The per-AP feature vectors are then concatenated to form the overall feature vector $\mathbf{F} \in \mathbb{R}^{8I}$.

We employ a MLP-based NN to predict the positioning error associated with every ambiguity pair. Let $e_{a,b}$ denote the ground-truth positioning error computed for the ambiguity pair $(\Delta z_a, \Delta z_b)$ using a pre-trained hyperbola intersection model. The network takes the feature vector \mathbf{F} as input and predicts these errors via $\hat{\mathbf{e}} = f_{\theta}(\mathbf{F}) \in \mathbb{R}^{\eta}$, where $f_{\theta}(\cdot)$ denotes the mapping implemented by the NN with trainable parameters θ , and each element $\hat{e}_{a,b}$ corresponds to the predicted positioning error for $(\Delta z_a, \Delta z_b)$. Here, $\eta = \binom{I-1}{2}$ denotes the total number of pairs that can be formed from $I-1$ ambiguities. The optimal pair for a given input is then selected as $(a^*, b^*) = \arg \min_{(a,b)} \hat{e}_{(a,b)}$. The NN architecture consists of an input layer of size $8I$, followed by five hidden layers with sizes $A, 2A, 4A, 2A$, and A , respectively, and concludes with an output layer of dimension $\binom{I-1}{2}$. The input and hidden layers employ the Rectified Linear Unit (ReLU) activation function, while the output layer uses a linear activation. Given a training set $\{(\mathbf{F}^{(i)}, \mathbf{e}^{(i)})\}_{i=1}^N$ with N samples, where $\mathbf{e}^{(i)}$ contains the ground-truth positioning errors for all pairs, the network is trained by minimizing the mean-squared error (MSE) loss function expressed as $\frac{1}{N} \sum_{i=1}^N \|\hat{\mathbf{e}}^{(i)} - \mathbf{e}^{(i)}\|^2$.

4. INFERENCE COMPLEXITY

We next evaluate the inference complexities of the proposed AP selection method and the hyperbola intersection approach. For a fair comparison with [13], the same complexity metric is adopted—namely, the floating-point operation (FLOP) count—where each elementary arithmetic operation is counted as one FLOP.

A fully connected (FC) layer with input and output sizes n_i and n_o requires approximately $2n_o n_i$ FLOPs. Since the proposed AP selection model consists solely of FC layers, its complexity is $\mathcal{C}_{\text{APS}} \approx 2A(20A + 8I + \eta)$ FLOPs. As reported in [13], the hyperbola intersection method has complexity $\mathcal{C}_{\text{HI}} = \mathcal{C}_{\text{DAE}} + \mathcal{C}_{\text{GD}}$, where the differential ambiguity estimator incurs $\mathcal{C}_{\text{DAE}} \approx D^2(4|\mathcal{J}| + 16) + D(2Q + 4I)$ FLOPs, and the GD-based solver requires $\mathcal{C}_{\text{GD}} \approx T(18|\mathcal{J}| + 10)$ FLOPs. When estimating only two ambiguities rather than all, both $|\mathcal{J}|$ and Q decrease, which reduces \mathcal{C}_{DAE} and \mathcal{C}_{GD} . However, for the overall complexity to be reduced, this decrease must outweigh the additional cost of \mathcal{C}_{APS} .

5. SIMULATION RESULTS

In our simulations, a 100 m^2 square region is used as the evaluation area, comprising $I = 9$ distributed APs arranged to

emulate a D-MIMO network topology. The AP locations are identical to those in [13], resulting in a total of $Q = 334$ possible output classes for all differential ambiguities. When the AP selection model is active and only two ambiguities are estimated, Q varies with the chosen ambiguity pair. To account for this, $Q/4$ is used, with the factor of 4 representing $\frac{I-1}{2}$. The 5G NR sounding reference signal (SRS)-based uplink pilot configuration and noise settings are identical to those in [13], while only a 0 dBm uplink transmit power level is considered in this work. The GD-based solver is set to perform $T = 500$ iterations using a learning rate of $\alpha = 0.08$.

5.1. Training of Proposed Neural Networks

The supervised training procedure involves two steps. First, we train the differential ambiguity estimator in the hyperbola intersection method to investigate the effect of the phase perturbations on the ambiguity estimation accuracy and to produce the correct ambiguity pair $(\Delta z_a, \Delta z_b)$ for each training sample of the AP selection network. During the training of the differential ambiguity estimator, all parallel branches are activated, i.e., no AP selection is applied. The neuron parameter is set to $D = 150$. This value is increased from 128 in [13] to 150 to preserve high ambiguity estimation accuracy in the presence of phase disturbances. The estimator is trained using 700×10^3 samples for training and 150×10^3 samples for validation, with UE positions, noise, and phase perturbations randomly sampled for each instance.

Second, we train the AP selection network. The neuron parameter is set to $A = 100$. Training of the AP selection model requires computing the positioning error for every ambiguity pair $(\Delta z_a, \Delta z_b)$ using the pre-trained hyperbola intersection model. Specifically, for each training instance, a random UE location, noise and phase perturbation realizations are generated first. The corresponding feature matrix \mathbf{F} is then constructed. For each ambiguity pair, the hyperbola intersection method is applied to obtain the UE positioning error, which serves as the ground-truth label for supervised learning. Using this procedure, 200×10^3 samples are employed for training, 40×10^3 for validation, and another 40×10^3 for testing.

5.2. Inference Complexity Reduction

With the considered parameters, the inference complexity of the AP selection model is $\mathcal{C}_{\text{APS}} \approx 0.420 \times 10^6$ FLOPs. For the hyperbola-intersection model, the inference complexity is $\mathcal{C}_{\text{HI,all}} \approx 1.262 \times 10^6$ FLOPs when all ambiguities are used, and $\mathcal{C}_{\text{HI,2}} \approx 0.594 \times 10^6$ FLOPs when only two ambiguities are used. By using two ambiguities in combination with the AP selection model instead of all ambiguities, the overall positioning complexity is reduced by approximately 19.7%.

5.3. Differential Ambiguity Estimation Results

We analyze the accuracy of the differential ambiguity estimator for all ambiguities, i.e., $|\mathcal{J}| = I - 1$. The *overall accuracy* is used as a performance metric. It is defined over S test samples as $A_o = \frac{1}{S} \sum_{s=1}^S \mathbb{I}(\Delta \hat{z}^s = \Delta z^s) \times 100\%$, where $\mathbb{I}(\cdot)$ denotes

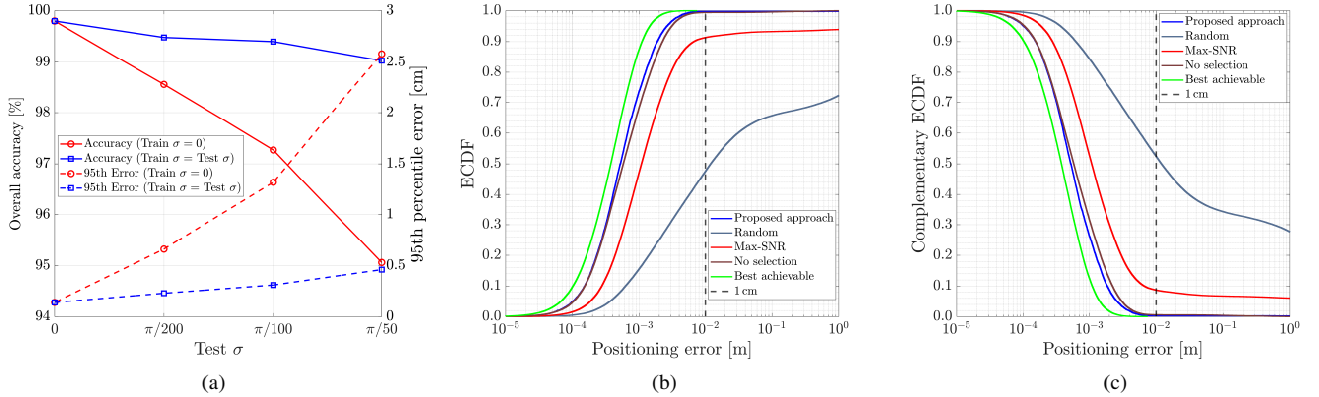


Fig. 3: (a) Accuracy and positioning performance with different training and test set combinations; (b) ECDF of the proposed approach and benchmarks; (c) complementary ECDF of the proposed approach and benchmarks.

the indicator function, which equals 1 when its argument is true and 0 otherwise. Here, $\Delta\hat{z}^s$ and Δz^s represent the estimated and ground-truth differential ambiguity vectors for the s -th test sample, respectively. Additionally, the 95th percentile positioning error is evaluated using the GD-based solver with all estimated ambiguities. To assess the model’s ability to adapt to different levels of phase perturbation, separate models are trained using phase perturbation standard deviation σ selected from $\{0, \pi/200, \pi/100, \pi/50\}$ and subsequently tested on distinct datasets. The results are illustrated in Fig. 3a, based on a test set containing $S = 150 \times 10^3$ samples.

When both the training and test sets include phase-perturbed data, increasing the perturbation has less impact on the overall accuracy and positioning performance compared with the case where the model is trained without phase perturbations. In the phase-perturbed training scenario, the overall accuracy remains above 99%, and the 95th-percentile error stays below 0.5 cm. This demonstrates that the model can adapt to phase perturbations and still achieve highly accurate positioning.

5.4. AP Selection Results

Since AP selection for phase-only positioning in D-MIMO has not been previously evaluated, there are no directly comparable benchmark methods available in the literature. We thus compare our AP selection method against the following four reference strategies: *Random* [15, 16], where the pair of ambiguities is chosen uniformly at random; *Max-SNR* [15, 17], where the pair of APs having the largest SNR values is chosen for differential ambiguity estimation; *No selection*, which uses all available ambiguities without AP selection; and *Best achievable*, representing the ground-truth subset with two ambiguities that yields the minimum positioning error for each test sample. The perturbation parameter σ in both the training and test sets is set to $\pi/100$. Fig. 3b shows the empirical cumulative distribution function (ECDF), i.e., $P\{\text{Positioning error} \leq x\}$, while Fig. 3c shows the comple-

Table 1: Positioning performance comparison of the considered AP selection models.

Method	Error [cm]	
	95th Perc.	99th Perc.
Best achievable	0.14	0.23
Proposed	0.26	0.48
No selection	0.30	0.59
Max-SNR	509.8	1057.4
Random	551.1	768.7

mentary ECDF, i.e., $P\{\text{Positioning error} > x\}$. The 95th and 99th percentile errors are compared in Table 1. The proposed AP selection model outperforms the *Max-SNR*, *Random*, and *No selection* benchmarks, and requires approximately 19.7% fewer FLOPs. Furthermore, considering the severe accuracy degradation observed in the *Max-SNR* and *Random* benchmarks, it can be concluded that, even when the model does not select the optimal pair, it effectively avoids the worst choices. Extremely low positioning errors such as $10 \mu\text{m}$ are observed when the AP and UE positions are perfectly measured during training; the impact of AP position uncertainties will be investigated in future work.

6. CONCLUSION

This paper demonstrated that carrier phase–only positioning, when combined with DL–based solutions, can achieve high-precision localization in realistic D-MIMO deployments. By explicitly addressing phase synchronization errors, the proposed DLMF framework enhances robustness against practical impairments while retaining centimeter-level accuracy. Moreover, the integration of adaptive AP selection strategies ensures efficient use of network resources. These results highlight the potential of phase-only positioning and learning-driven approaches as key enablers for reliable and accurate localization in future 6G systems. Future work will extend the proposed framework to cover multipath and three-dimensional scenarios.

7. ACKNOWLEDGMENTS

This work was supported by the MiFuture project under the HORIZON-MSCA-2022-DN-01 call (Grant number: 101119643), by the SNS JU project 6G-DISAC under the EU's Horizon Europe research and innovation Program under Grant Agreement No 101139130, and by the Swedish Research Council (VR) through the project 6G-PERCEF under Grant 2024-04390. The work was also in part supported by Business Finland under the 6G-ISAC project, and in part by the Research Council of Finland under the grant 359095.

8. REFERENCES

- [1] H.-S. Cha, G. Lee, A. Ghosh, M. Baker, S. Kelley, and J. Hofmann, “5G NR positioning enhancements in 3GPP release-18,” *IEEE Commun. Stand. Mag.*, vol. 9, no. 1, pp. 22–27, 2025.
- [2] J. Nikonorowicz, A. Mahmood, M. I. Ashraf, E. Björnson, and M. Gidlund, “Indoor positioning in 5G-Advanced: Challenges and solution toward centimeter-level accuracy with carrier phase enhancements,” *IEEE Wireless Commun.*, vol. 31, no. 4, 2024.
- [3] S. Fan, W. Ni, H. Tian, Z. Huang, and R. Zeng, “Carrier phase-based synchronization and high-accuracy positioning in 5G new radio cellular networks,” *IEEE Trans. Commun.*, vol. 70, no. 1, pp. 564–577, 2022.
- [4] N. González-Prelcic, M. Furkan Keskin, O. Kaltiokallio, M. Valkama, D. Dardari, X. Shen, Y. Shen, M. Bayraktar, and H. Wymeersch, “The integrated sensing and communication revolution for 6G: Vision, techniques, and applications,” *Proc. IEEE*, vol. 112, no. 7, pp. 676–723, 2024.
- [5] J. Talvitie, M. Säily, and M. Valkama, “Orientation and location tracking of XR devices: 5G carrier phase-based methods,” *IEEE J. Sel. Topics Signal Process.*, vol. 17, no. 5, pp. 919–934, 2023.
- [6] Y. Wu, M. F. Keskin, U. Gustavsson, G. Seco-Granados, E. G. Larsson, and H. Wymeersch, “Location and map-assisted wideband phase and time calibration between distributed antennas,” in *IEEE Globecom Workshops (GC Wkshps)*, 2024, pp. 1–6.
- [7] Ö. T. Demir, E. Björnson, and L. Sanguinetti, “Foundations of user-centric cell-free massive MIMO,” *Found. Trends Signal Process.*, vol. 14, no. 3-4, pp. 162–472, 2021.
- [8] E. G. Larsson, “Massive synchrony in distributed antenna systems,” *IEEE Trans. Signal Process.*, vol. 72, pp. 855–866, 2024.
- [9] K. Trichias, A. Kaloxyllos, and C. Willcock, “6G global landscape: A comparative analysis of 6G targets and technological trends,” in *EuCNC & 6G Summit*, 2024, pp. 1–6.
- [10] A. Pinto, G. Santaromita, C. Fiandrino, D. Giustiniano, and F. Esposito, “Characterizing location management function performance in 5G core networks,” in *IEEE Conf. Netw. Funct. Virtualiz. Softw. Defin. Netw.*, 2022, pp. 66–71.
- [11] A. Pauwels, I. Franco, L. Bertrand, M. Vuong, J. Chang, and T. W. Spicer, “Distributed location management function for positioning in wireless networks,” Patent US20 200 367 022A1, November, 2020, published Nov. 26, 2020; Filed May 15, 2020.
- [12] F. Ayten, M. C. Ilter, O. Kaltiokallio, J. Talvitie, A. Jain, E. S. Lohan, H. Wymeersch, and M. Valkama, “Phase-only positioning: Overcoming integer ambiguity challenge through deep learning,” in *IEEE 36th Int. Symp. on Personal, Indoor and Mobile Radio Commun. (PIMRC)*, 2025, pp. 1–7.
- [13] F. Ayten, M. C. Ilter, A. Jain, O. Kaltiokallio, J. Talvitie, E. S. Lohan, H. Wymeersch, and M. Valkama, “Failure tolerant phase-only indoor positioning via deep learning,” in *IEEE 36th Int. Symp. on Personal, Indoor and Mobile Radio Commun. (PIMRC)*, 2025, pp. 1–7.
- [14] A. Fascista, B. J. B. Deutschmann, M. F. Keskin, T. Wilding, A. Coluccia, K. Witrisal, E. Leitinger, G. Seco-Granados, and H. Wymeersch, “Uplink joint positioning and synchronization in cell-free deployments with radio stripes,” in *Proc. IEEE Int. Conf. on Commun. Workshops (ICCW)*, 2023, pp. 1330–1336.
- [15] S. Biswas and P. Vijayakumar, “AP selection in cell-free massive MIMO system using machine learning algorithm,” in *Int. Conf. on Wireless Commun., Signal Processing and Netw. (WiSPNET)*, 2021, pp. 158–161.
- [16] J. Feng, Z. Guo, X. Wang, and X. Chen, “Reinforcement learning based AP selection in cell-free massive MIMO systems with phase-noise,” in *Int. Conf. on Future Commun. and Netw. (FCN)*, 2024, pp. 1–6.
- [17] Z. Deng, L. Ma, and Y. Xu, “Intelligent AP selection for indoor positioning in wireless local area network,” in *Int. ICST Conf. on Commun. and Netw. in China (CHINA-COM)*, 2011, pp. 257–261.